

Pharmacokinetic analysis of protein-conjugated doxorubicin (DXR) and its degraded adducts in DXR-sensitive and -resistant rat hepatoma cells

Naoto Takahashi, Tadashi Asakura and Kiyoshi Ohkawa

Department of Biochemistry (I), Jikei University School of Medicine, Tokyo 105, Japan.
Tel: (+81) 3-3433-1111; Fax: (+81) 3-3435-1922.

After treatment of AH66DR cells with the multidrug resistance (MDR) phenotype with bovine serum albumin (BSA)-conjugated [14 C]doxorubicin (DXR), accumulation of the drug in the secondary lysosomal fraction increased as a function of time up to 24 h without any significant increase of the drug in other organelles. By contrast, AH66P cells showed a marked increase in accumulation of the drug in the mitochondrial fraction, and a moderate increase in the lysosomal and nuclear fractions. The intracellular degradation of the internalized conjugate was assessed by HPLC gel filtration as molecular change of the drug. The initial molecular mass (M_r) of BSA-conjugated [14 C]DXR was estimated to be 70 kDa; however, the secondary lysosomal fraction contained mainly three peaks of [14 C]compounds ranging from 3 to 70 kDa. The [14 C]compound extracted from the nuclear and mitochondrial fractions showed only one peak, which was estimated to be smaller than 2 kDa. By contrast, the cytosolic fraction contained mainly two peaks of [14 C]compounds, which were smaller than 2 kDa and larger than 500 kDa. These results indicated that the intracellular distribution of the administered drug, based probably on the drug-traffic mechanism in the cells, was quite different between the two cell lines, but some of the biochemical characteristics of the degraded compounds from each subcellular fraction were similar because the degradation processes in each fraction might be almost identical. The possibility of lysosomal degradation of the protein-conjugated DXR leading to expression of cytotoxicity was also confirmed by the fact that only lysosomal digestible poly-L-lysine-conjugated DXR exhibited dose-dependent cytotoxicity against both cell lines in marked contrast to the cells treated with poly-D-lysine-conjugated DXR. It was concluded that lysosomal breakdown of protein-conjugated DXR, which had been taken up by endocytosis, and the liberation of the degraded active adducts of the conjugate without efflux by the MDR pump mechanism must be an essential stage in the development of the cytotoxicity against tumor cells with or without the MDR phenotype.

Key words: Doxorubicin, gel filtration, HPLC, multidrug resistance, protein-conjugated doxo-rubicin, rat hepatoma.

Introduction

The appearance of multidrug resistance (MDR) to antitumor drugs through the overexpression of transmembrane 170 kDa P-glycoprotein (Pgp) is a major problem in cancer chemotherapy.^{1,2} Various attempts to overcome MDR have been studied, including co-treatment with a calcium antagonist to block the efflux pump of Pgp^{3–5} and the use of anti-Pgp monoclonal antibody to modulate the MDR phenotype.^{6–8} We have recently reported that protein-conjugated doxorubicin (DXR) exhibited a marked cytotoxicity against several MDR cell lines.^{9–11} The reports demonstrated that the conjugate was slowly internalized, but not pumped out by Pgp, resulting in increased accumulation and improved cytotoxicity. A mechanism proposed to explain the main antitumor activity of DXR is the inhibition of DNA replication by intercalation of DNA base pairs, but the mechanism of cytotoxicity of the protein-conjugated DXR on the MDR cells has not yet been clarified. Anticancer agents, for the most part, exert their cytotoxic effects through interaction with their intracellular target component; the antitumor effects are dependent on the active drugs that are taken up by cells. Thereafter, internalization of the protein-conjugated DXR, intracellular translocation of the protein-conjugated DXR and the release of the agent into a pharmacologically active form within the cells are critical processes in determining the cytotoxic effect of the protein-conjugated DXR. In the present study, to clarify the mechanism(s) by which the protein-conjugated DXR overcomes MDR, the characteristics of the intracellular distribution and the degradation of bovine serum albumin (BSA)-conjugated DXR were investigated using both DXR-sensitive and -resistant cell lines.

This work was supported in part by Grant-in-Aid for Scientific Research from the Ministry of Education, Science and Culture, Japan, and by a grant from the Sankyo Foundation of Life Science.

Correspondence to K Ohkawa

Materials and methods

Materials

DXR was obtained from Kyowa Hakko Kogyo Co., Ltd (Tokyo, Japan). Dextran T-10, and Sephadex G-25 and G-150 were obtained from Pharmacia Biotech (Uppsala, Sweden). BSA, catalase, ribonuclease I, DNA from calf thymus, poly-L-lysine (MW 53.9 kDa), poly-D-lysine (MW 55.0 kDa), ethidium bromide, goat anti-BSA polyclonal antibody, fluorescein isothiocyanate (FITC)-labeled rabbit anti-mouse immunoglobulin, FITC-labeled rabbit anti-goat immunoglobulin and 3-(4,5-dimethyl-2-thiazolyl)-2,5-diphenyl-tetrazolium bromide (MTT) were obtained from Sigma (St Louis, MO). Mouse anti-DXR monoclonal antibody was generated by immunizing mice with keyhole limpet hemocyanin-DXR conjugate as reported previously.¹² [¹⁴C]DXR (57 mCi/mmol) was purchased from Amersham Japan (Tokyo, Japan). Molecular weight standard of multiples of a 123 bp DNA ladder was obtained from Gibco/BRL (Gaithersburg, MD). 3,5-Diaminobenzoic acid, Triton X-100 and agarose GP-36 were obtained from Nakarai Tesque Inc. (Kyoto, Japan). All other chemicals were of analytical grade.

Cell lines

The rat ascites hepatoma cell line, AH66P, and the DXR-resistant mutant subline, AH66DR, were cultured with RPMI 1640 containing 10% heat inactivated fetal bovine serum (growth medium) under the conventional conditions.¹⁰

Preparation of DXR conjugated with protein

Binding of DXR to BSA via a dextran bridge was carried out using a method described previously.¹³ Briefly, 10 mg/0.5 ml in 0.15 M NaCl of oxidized dextran T-10 which was linked with [¹⁴C]DXR at room temperature for 1 h was coupled with 10 mg of BSA at 4°C for 24 h. The BSA-conjugated [¹⁴C]DXR was separated from unbound [¹⁴C]DXR by Sephadex G-150 gel filtration. For the preparation of DXR conjugated with poly-lysine, mixtures of 3 mg of poly-L-lysine or poly-D-lysine and 0.5 mg of DXR in 1 ml of 0.15 M NaCl containing 0.1% glutaraldehyde were incubated for 15 min at room temperature. The conjugate was separated from free DXR by Sephadex G-25 gel filtration.⁹⁻¹¹ The concentration of DXR was

measured by absorbance at 495 nm. Protein concentration was estimated by the measurement of absorbance at 280 nm or by the ninhydrin reaction.

Fluorescence study

After the cells were co-cultured for 10 min, 1 h and 17 h with 10 μ M DXR or BSA-conjugated DXR at equivalent DXR doses, the cells were incubated with prewarmed 10 mM sodium phosphate buffer, pH 7.0, 0.15 M NaCl (PBS) containing 10 mM NaN₃ for 15 min. The cells that had been washed extensively with the cold buffer mentioned above were fixed by cold acetone for 1 min. Next, the intracellular drug distribution was examined by the immunofluorescence antibody method using mouse anti-DXR monoclonal antibody, goat anti-BSA polyclonal antibody and FITC-labeled second antibody. DXR fluorescence was also detected by fluorescence microscopy (Olympus LH5A; Olympus Optical Co. Ltd, Tokyo, Japan).

Uptake of DXR or protein-conjugated DXR

AH66P or AH66DR (5×10^4) cells were cultured in the presence of 1 nM [¹⁴C]DXR or BSA-conjugated [¹⁴C]DXR in culture plates (no. 3003; Falcon, Becton Dickinson, Lincoln Park, NJ). After incubation for various periods of time, the media were removed and the scraped cells were washed three times with 3 ml of ice-cold 0.15 M NaCl. The level of intracellular drug was estimated by the measurement of radioactivity using a scintillation counting system (LS6000IC; Beckman, Berkeley, CA). For the uptake of poly-lysine-conjugated DXR, the scraped and washed cells, which were incubated with 5 μ M isomeric poly-lysine-conjugated DXR for 24 h, were sonicated mildly in 10 mM Tris-HCl, pH 7.4, and one-eighth volumes of 2 M sucrose were added to the suspensions, which were then centrifuged at 1000 g for 10 min to obtain the pellet (P1) and supernatant (S1). The nuclear fraction was isolated from P1 using sucrose discontinuous centrifugation as described by Tata *et al.*¹⁴ The nuclear fraction and S1 were combined and mixed with the same volumes of 2% Triton X-100. DXR in the mixture was measured by fluorospectrometry set at an emission wavelength of 470 nm with an excitation wavelength of 580 nm using authentic DXR as a standard. The results were expressed by the following equation: drug accumulation rate (%) = $100 \times [\text{intracellular DXR (nmol) per } 5 \times 10^4 \text{ cells}]/[\text{DXR (nmol) added to medium}]$.

Subcellular fractionation

Subcellular particles from AH66P and AH66DR cells were fractionated by differential centrifugation after treatment of the cells with [^{14}C]DXR or with BSA-conjugated [^{14}C]DXR for various periods of time. All procedures were carried out at 4°C. P1, S1 and nuclear fractions were prepared from the cells as described above. S1 was further centrifuged at 10 000 g for 20 min to obtain the pellet (P2) and supernatant (S2) fractions. P2 suspended in 0.7 M sucrose–0.2 M KCl was centrifuged at 10 000 g for 10 min. The resultant pellet was used as a mitochondrial fraction and a primary lysosomal fraction was obtained from the supernatant by centrifugation at 15 000 g for 20 min. A secondary lysosomal fraction containing endosomes was precipitated from S2 by centrifugation at 20 000 g for 30 min. The consequent supernatant was used as a cytosolic fraction. Subcellular accumulation of [^{14}C]drugs was expressed as radioactivity (d.p.m.)/mg protein in each fraction. To determine the intercalated BSA-conjugated [^{14}C]DXR into DNA, the DNA fraction of AH66P and AH66DR cells treated with the drugs was extracted with phenol from the nuclear fraction and precipitated by ethanol. The accumulation of radioactivity in DNA was expressed as d.p.m./mg DNA.

DNA fragmentation assay

To determine whether both cells treated with BSA-conjugated DXR displayed typical apoptotic features, the appearance of typical oligonucleosomal base pair fragments was examined in the drug-treated tumor cells. After treatment with the drug for various periods of time, harvested cells (1×10^7) were centrifuged and washed with cold PBS. DNA was extracted from the cells by the IsoQuick Nucleic Acid Extraction Kit (Microprobe, Garden Grove, CA). The DNA precipitated by ethanol was dissolved in 50 μl of 10 mM Tris–HCl (pH 7.5) containing 1 mM EDTA. The DNA sample (10 μg) was loaded on 2% agarose gels. After electrophoresis, the DNA fragments were visualized by ethidium bromide staining and the gels were photographed.

Estimation of molecular mass (M_r) of the internalized BSA-conjugated [^{14}C]DXR in the subcellular fraction

After 24 h of treatment of both AH66P and AH66DR cells with BSA-conjugated [^{14}C]DXR, lysosomal, cyto-

solic, nuclear and mitochondrial fractions were separated by differential centrifugation as described above. M_r estimation of ^{14}C compounds in respective fractions was performed by HPLC gel filtration (TSK gel G3000SW, 7.5×600 mm; Tohso, Tokyo, Japan). Elution was carried out with 0.15 M NaCl at a flow rate of 1 ml/min. The radioactivity in each fraction was measured by the scintillation counting system. The molecular size markers used were catalase (240 kDa), BSA (66 kDa) and ribonuclease I (13 kDa).

Growth inhibitory effect of poly-L-lysine- and poly-D-lysine-conjugated with DXR

To assess the growth inhibitory effect of drugs, viable cells (2×10^4) were cultured continuously for 96 h at 37°C in a 48-well culture plate (no. 3548; Costar, Cambridge, MA) with 1 ml of growth media containing graded equivalent concentrations of DXR or poly-lysine. After 96 h incubation, viable cells were determined with the colorimetric assay using MTT as reported previously¹⁵ and the results were expressed by the following equation: viable cells (%) = $100 \times (\text{absorbance at 570 nm of the drug-exposed cells}) / (\text{absorbance at 570 nm of the non-treated control cells})$.

Protein and DNA assay

Protein concentration in each subcellular fraction was determined by a Bio-Rad protein assay kit (Bio-Rad, Hercules, CA) using BSA as the standard. DNA concentration was assayed as follows: DNA extracted from the cells was mixed with 0.1 ml of 2 M 3,5-diaminobenzoic acid and incubated at 60°C for 30 min. After incubation, 4 ml of 0.6 M perchloric acid was added to the mixture. The binding product of DNA with 3,5-diaminobenzoic acid was measured by fluorospectrometry set at an emission wavelength of 515 nm with an excitation wavelength of 415 nm using DNA from calf thymus as the standard.¹⁶

Results

DXR conjugates with protein

The extent of substitution varied in different preparations and the conjugates when 5.2 mol [^{14}C]DXR per mol BSA, 15 mol DXR per mol poly-L-

lysine and 16 mol DXR per poly-D-lysine, respectively, were used in the present study.

Fluorescence localization of BSA and DXR

To confirm the internalization and distribution of DXR and BSA-conjugated DXR in the cells, DXR immunolocalization was determined by the anti-DXR antibody immunofluorescence method (Figure 1). Although DXR immunoreactivity was detectable through the cytoplasm and nuclei of the AH66P cells within only 1 h of treatment (Figure 1A), little DXR was accumulated in the nuclei of AH66DR cells over 17 h of treatment (Figure 1B). By contrast, AH66DR treated with BSA-conjugated DXR for 17 h showed a significant immunodistribution of the drug through the cytoplasm and nuclei (Figure 1C). The distribution of BSA-conjugated DXR in AH66DR cells was investigated further using anti-BSA antibody and DXR fluorescence. After 10 min of treatment with BSA-conjugated DXR, both BSA and DXR were practically not detected in the cells (Figure 2A and D). Fluorescence were detected significantly around the perinuclear region after 1 h of treatment (Figure 2B and E). After 17 h of treatment, both fluorescence intensities were increased in the nuclei as well as in the cytoplasm (Figure 2C and F).

Cellular accumulation of BSA-conjugated DXR

As the uptake of [14 C]DXR into both AH66P and AH66DR cells was saturated after approximately 30 min of incubation, a comparison was made of the intracellular [14 C]DXR level between the two cell lines after 1 h of treatment. The accumulation of [14 C]DXR in AH66DR cells was only 13% of that in AH66P cells. On the other hand, the accumulation of BSA-conjugated [14 C]DXR in AH66P cells was found to be increased slowly up to 24 h of the treatment period and reached approximately the same level as that after 1 h of treatment with [14 C]DXR (equivalent concentration) (Figure 3). After treatment of AH66DR cells with BSA-conjugated [14 C]DXR for 24 h, the drug accumulation increased gradually and reached approximately 31% of the level in AH66P cells treated with the conjugate for 24 h (Figure 3). When both cells were treated with 5 μ M of either poly-L-lysine- or poly-D-lysine-conjugated DXR for 24 h, these drugs were

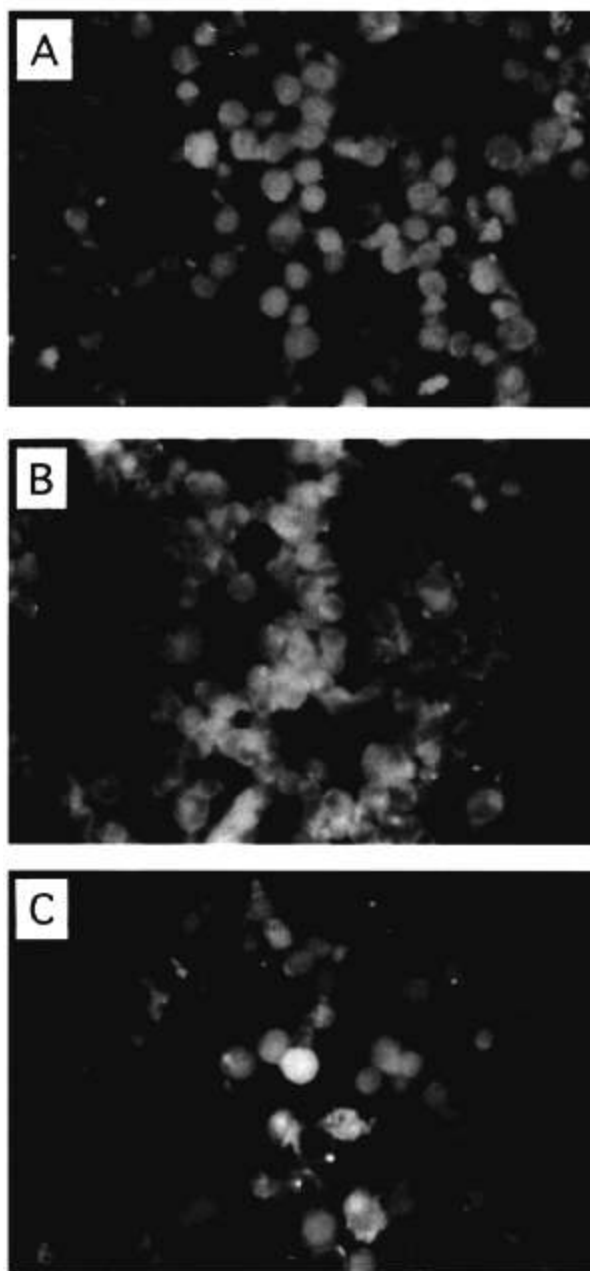


Figure 1. Analysis of drug distribution using fluorescence microscopy. After co-culture for 1 and 17 h with 10 μ M DXR or BSA-conjugated DXR at equivalent DXR doses, intracellular drug distribution was examined using mouse anti-DXR monoclonal antibody and FITC-labeled second antibody by an immunofluorescence method. (A) AH66P cells co-cultured with 10 μ M DXR for 1 h; (B and C) AH66DR cells co-cultured with 10 μ M DXR and with 10 μ M BSA-conjugated DXR for 17 h, respectively.

taken up into the cells. The drug accumulation rates for poly-L-lysine-conjugated DXR were $15.9 \pm 2.9\%$ in AH66P cells and $17.6 \pm 3.0\%$ in AH66DR cells, while the rates for poly-D-lysine-conjugated DXR

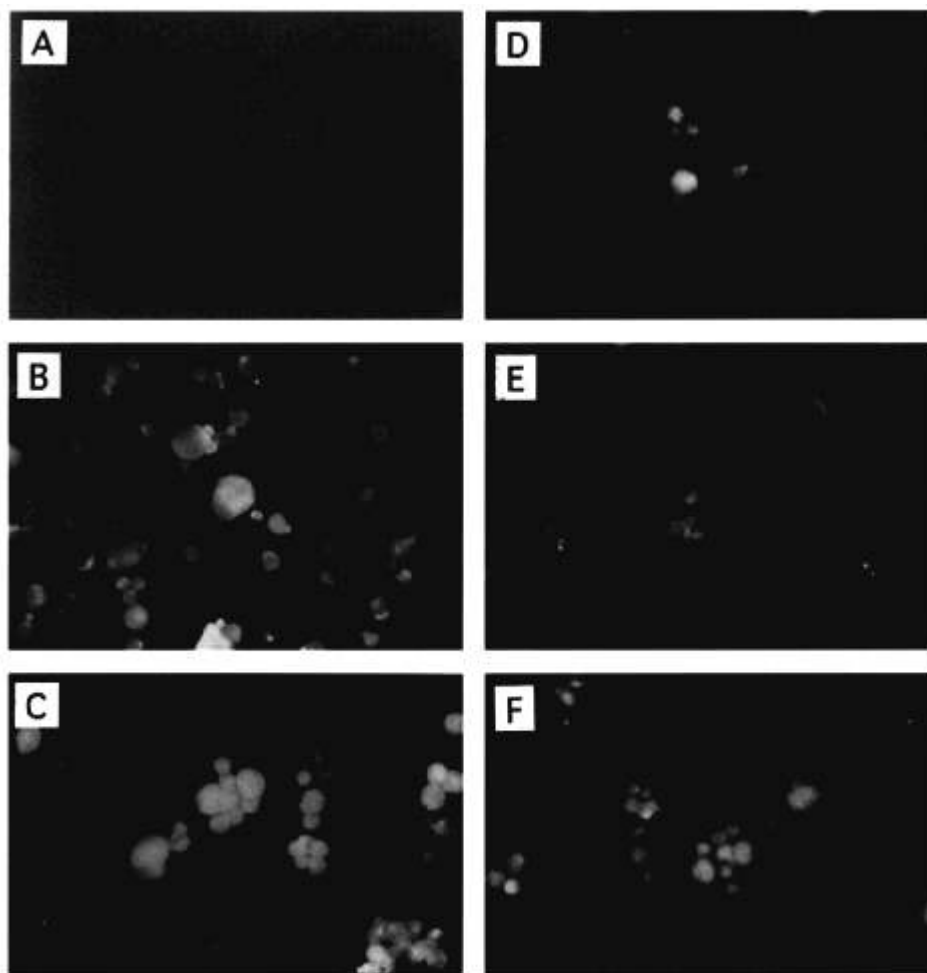


Figure 2. Distribution of BSA-conjugated DXR in AH66DR cells incubated in the presence of $10\ \mu\text{M}$ BSA-conjugated DXR for 10 min (A and D), 1 h (B and E) and 17 h (C and F). Intracellular drug distribution was examined using goat anti-BSA polyclonal antibody and FITC-labeled second antibody by an immunofluorescence method (A–C). DXR fluorescence was also detected by fluorescence microscopy (D–F).

were $21.1 \pm 3.9\%$ in AH66P cells and $16.6 \pm 3.8\%$ in AH66DR cells. These values did not show any significant differences between two kinds of conjugate or two cell lines.

Intracellular distribution of BSA-conjugated DXR

After incubation of the cells with BSA-conjugated [^{14}C]DXR for various periods of time, the time-dependent and organella-specific accumulations of [^{14}C]compounds were observed in nuclear, mitochondrial, secondary lysosomal and cytosolic fractions from either AH66P or AH66DR cells (Table 1). The separation of each fraction was confirmed using marker enzymes, such as succinate dehydrogenase

for mitochondria, acid phosphatase for lysosomes and lactate dehydrogenase for cytosol^{17–19} (data not shown).

Treatment of AH66P cells with BSA-conjugated [^{14}C]DXR resulted in the highest accumulation of radioactivity in the nuclear fraction. The cumulative radioactivity after 24 h of treatment was increased approximately 3-fold as compared with that after 1 h of treatment. The radioactivity in the mitochondrial fraction was also increased as a function of time up to 24 h and reached the highest level after 24 h of treatment. After 24 h of treatment, the intracellular drug distribution in AH66P cells which were treated with BSA-conjugated [^{14}C]DXR showed almost the same pattern as that of [^{14}C]DXR. In AH66DR cells, the intracellular drug distribution after 24 h of treatment with

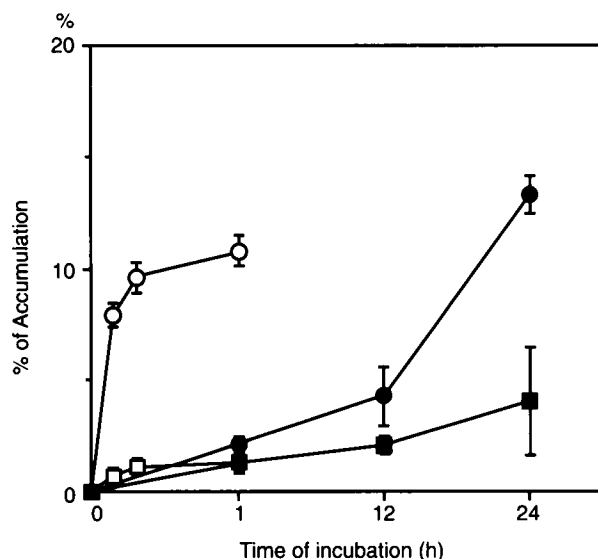


Figure 3. Time-dependent accumulation of the BSA-conjugated DXR in DXR-sensitive AH66P or -resistant AH66DR cells. After incubation with either free [^{14}C]DXR or BSA-conjugated [^{14}C]DXR, intracellular radioactivity was measured with a liquid scintillation counter. AH66P cells treated with BSA-conjugated [^{14}C]DXR (●) and with free [^{14}C]DXR (○). AH66DR cells treated with BSA-conjugated [^{14}C]DXR (■) and with free [^{14}C]DXR (□). Points: mean of duplicate determinations of three independent examinations; bars: SD.

BSA-conjugated [^{14}C]DXR had a nearly similar pattern to that of [^{14}C]DXR with the exception of low accumulation in the nuclear fraction. The secondary lysosomal accumulation of [^{14}C]compounds was increased gradually and reached the maximum concentration after 24 h of treatment. The nuclear and mitochondrial accumulations did not show any

significant increase over a 24 h time period as compared with the level after 1 h of treatment with BSA-conjugated [^{14}C]DXR. The radioactivity was practically not detected in the primary lysosomal fractions from both cell lines throughout the experiment (data not shown).

By treatment of the two cell lines with BSA-conjugated [^{14}C]DXR, the time-dependent increase in accumulation of the drug was not observed in the DNA fraction over a 24 h time period and they were almost at the same levels as that after 1 h of treatment. Drug accumulation in the nuclear fraction was lower in AH66DR cells than that in AH66P cells; however, the level of radioactivity of the drug in the DNA fraction, which was extracted from the same nuclear fraction, was interestingly higher in the AH66DR cells relative to that in AH66P cells. On the other hand, treatment of AH66DR cells with [^{14}C]DXR showed a much lower accumulation of the drug in DNA than that with BSA-conjugated [^{14}C]DXR.

Induction of DNA fragmentation by BSA-conjugated DXR

Because a time-dependent increase in the radioactivity was not observed in DNA fractions from both AH66P and AH66DR cell lines which were treated with BSA-conjugated [^{14}C]DXR as described above, it was investigated further whether or not the DNA fragmentation was induced by the treatment. When the cells were exposed to $1\ \mu\text{M}$ BSA-conjugated DXR for various periods of time, some nucleosome-sized fragments were expressed in both cell lines after 12 h of treatment (Figure 4).

Table 1. Subcellular distribution of the drugs in AH66P and AH66DR cells

Fraction	AH66P				AH66DR			
	BSA-conjugated DXR			DXR	BSA-conjugated DXR			DXR
	1 h	12 h	24 h		1 h	12 h	24 h	
Nuclei	5052	4931	15323	15325	1386	1379	1887	3810
Mitochondria	1449	3629	9864	10591	1298	1546	1414	1863
Second lysosomal	525	578	2062	3131	799	935	1815	1410
Cytosol	1053	963	2447	2319	955	911	1532	1246
DNA	1938	1327	1350	3318	1533	2015	1820	785

Subcellular distribution of the radioactivity in AH66P and AH66DR cells which were treated with BSA-conjugated [^{14}C]DXR or with free [^{14}C]DXR. After 1, 12 or 24 h of treatment of the cells with the drugs, the radioactivity of nuclear, mitochondrial, secondary lysosomal, cytosolic fractions and DNA was measured with a liquid scintillation counter ($n = 2$, mean). For details, see Materials and methods. Results are expressed as radioactivity (d.p.m.)/mg protein or mg DNA in each fraction.

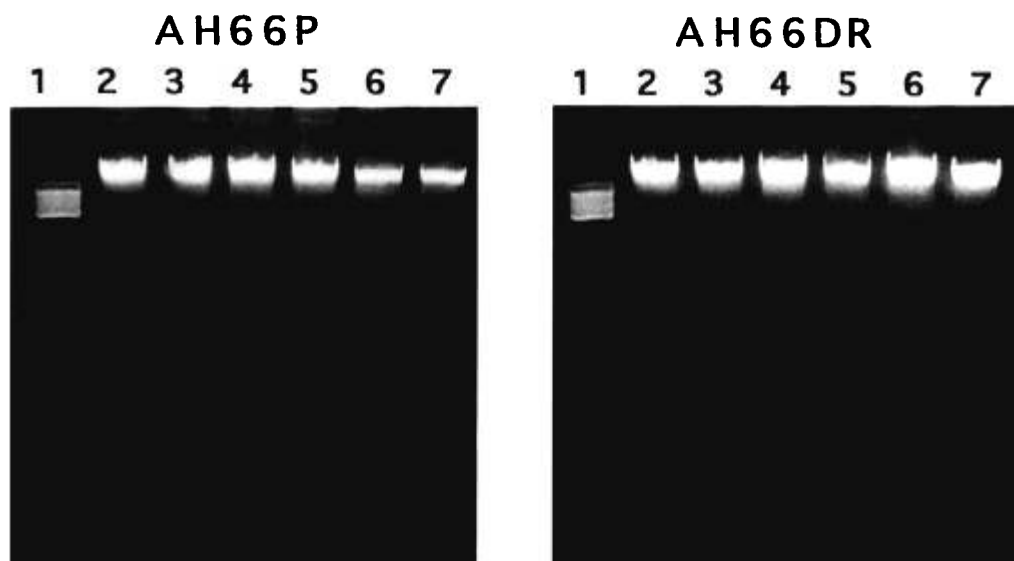


Figure 4. Induction of DNA fragmentation by BSA-conjugated DXR. After drug treatment, isolated DNA was electrophoresed in a 2.0% agarose gel as described in the Materials and methods. Both cells (A, AH66P; B, AH66DR) were treated with 1 μ M BSA-conjugated DXR for various periods of time (lane 2, control; lane 3, 3 h; lane 4, 6 h; lane 5, 12 h; lane 6, 24 h; lane 7, 30 h). Molecular weight standards of multiples of the 123 bp DNA ladder are shown in lane 1.

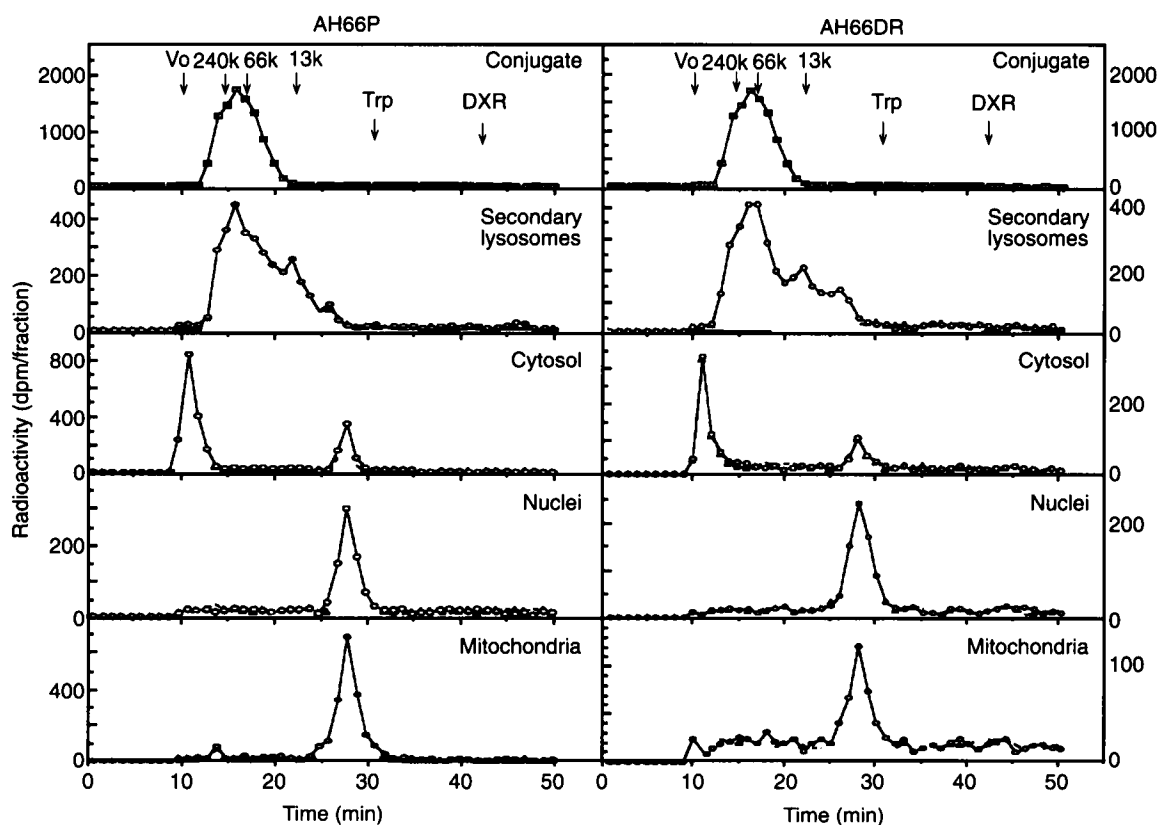


Figure 5. Estimation of M_r of the internalized [14 C]DXR conjugate in the subcellular fraction. After 24 h of treatment of both AH66P and AH66DR cells with BSA-conjugated [14 C]DXR, secondary lysosomal, cytosolic, nuclear and mitochondrial fractions were separated by differential centrifugation as described in Materials and methods. M_r distribution of 14 C compounds in respective fractions was estimated by HPLC gel filtration (G3000SW). Elution was carried out with 0.15 M NaCl at a flow rate of 1 ml/min. The radioactivity of each fraction was measured by the scintillation counting system.

M_r changes of the internalized BSA-conjugated [^{14}C]DXR

As shown in Figure 5, M_r of the BSA-conjugated [^{14}C]DXR initially prepared was estimated to be approximately 70 kDa. In AH66P cells, the internalized BSA-conjugated [^{14}C]DXR was degraded in the secondary lysosomes and the [^{14}C]compounds in the fraction were separated mainly into three peaks ranging from 3 and 70 kDa. By contrast, the M_r of [^{14}C]compounds which were extracted from the nuclear and mitochondrial fractions were estimated to be only smaller than 2 kDa. The cytosolic fraction contained two peaks smaller than 2 kDa and larger than 500 kDa of [^{14}C]compounds. Free [^{14}C]DXR was not detectable in any fraction. In AH66DR cells, the elution profile of the internalized conjugate in each subcellular fraction was almost similar to that in AH66P cells obtained by HPLC gel filtration analysis.

Cytotoxicity against isomeric poly-lysine-conjugated DXR

To investigate whether lysosomal enzymes contribute to expression of the cytotoxicity of the conjugate, both poly-L-lysine and poly-D-lysine were used as the partner of the conjugate instead of BSA.²⁰ Only poly-L-lysine-conjugated DXR exhibited a growth inhibitory effect in a dose-dependent manner against both cells in marked contrast to the cells treated with poly-L-lysine-, poly-D-lysine- and poly-D-lysine-conjugated DXR, respectively (Figure 6).

Discussion

Distribution of DXR and BSA-conjugated DXR in the cells was determined by either immunofluorescence or DXR-fluorescence. Treatment of the DXR-resistant AH66DR cells with BSA-conjugated DXR for 17 h showed a significant distribution of the drug in the cytoplasm and nuclei, whereas no obvious distribution of the DXR was noted in the AH66DR nuclei within the same period of time. These results indicated the internalization of BSA-conjugated DXR in the cytoplasm, because both DXR and BSA were detected clearly in the cells by fluorescence microscopy.

By pharmacokinetic analysis of [^{14}C]DXR conjugated with BSA, an obvious difference in mitochondrial and nuclear accumulations of the conjugate was found between AH66P and AH66DR cells.

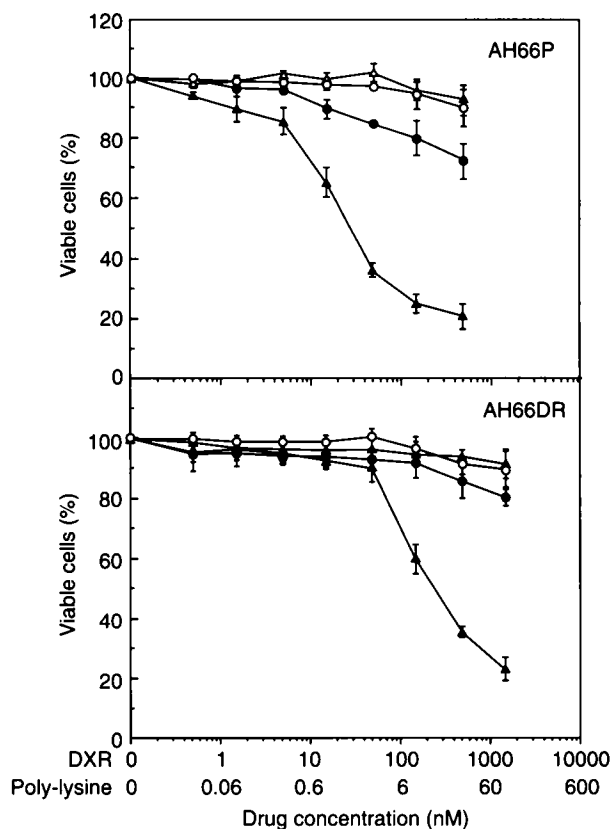


Figure 6. The cytotoxic effect of poly-lysine at various concentrations and poly-lysine-conjugated DXR at the equivalent concentration of DXR on AH66P or AH66DR cells was examined using the MTT assay in terms of percentage of viable cells relative to the control. Each cell line was treated with poly-L-lysine-conjugated DXR (▲), poly-D-lysine-conjugated DXR (●), poly-L-lysine (△) or poly-D-lysine (○). Mean \pm SD (four examinations).

Accumulation of the drug in the nuclei of AH66DR cells was lower than that of AH66P cells because of the active DXR efflux from nucleus to cytoplasm and from cytoplasm to outside the cells.²¹ In this condition, approximately 20% of the DXR, which had been accumulated in the nuclear fractions of both DXR sensitive and -resistant cells, was extracted in the DNA fraction. By contrast, nuclear accumulation of the BSA-conjugated DXR in both cell lines was very slow as compared to that of free DXR because of their different mechanisms of influx. In AH66DR cells, the internalized BSA-conjugated DXR was degraded and the resultant adducts were distributed to the target organelles, such as the nucleus and mitochondria. However, we have already detected over 30–40% of the metabolic adducts of the conjugate that were also effluxed from the cells by the Pgp pump (manuscript in preparation). This explains why nuclear accumulation of the BSA-

conjugated DXR was lower in the AH66DR cells than that in AH66P cells. Under this condition, the accumulated conjugate or its metabolic adduct in the nuclear fraction of the AH66DR cells was almost entirely bound to DNA and the accumulation of the drug in the DNA fraction, which was extracted from the nuclear fraction, was the same or higher in concentration as compared to the drug level exhibiting excellent cytotoxicity when the AH66P cells were treated with the conjugate. We presume from this result that the level of the drug intercalated into DNA was sufficient to exhibit cytotoxicity against AH66DR cells as well as AH66P cells. A lack of time-dependent accumulation of the drug in DNA may be based on the simultaneous transportation out of the nuclei of the DNA fragment which was generated by the drug action. In the present study, the internucleosomal cleavage of genomic DNA occurred in both cell lines after 12 h of treatment with BSA-conjugated DXR. Extraction of the drug from DNA is dependent on certain factors, such as drug-binding strength, drug hydrophobicity, etc. Formation of an unknown drug-DNA-protein complex, cleavable complex or resultant fragmentation of the DNA may also affect the efficiency of the extraction process of DXR from DNA since DNA damage in the tumor cells induced by DXR was mediated in part by DNA topoisomerase II.²² It has been reported that both levels of DNA topoisomerase II mRNA and protein were decreased in MDR cells relative to the parent cells.^{23,24} The effect of BSA-conjugated DXR on enzyme activity and expression of DNA topoisomerase I or II is now under investigation.

The higher accumulation of the conjugate was also observed in the mitochondrial fraction from AH66P cells in comparison with that from AH66DR cells. Mitochondrial accumulation of the drug may increase cytotoxicity due to the production of reactive oxygen species, in particular the hydroxy radical, which cleaves DNA.²⁵⁻²⁷ This phenomenon may be one of the reasons why the conjugate exhibited superior cytotoxicity against the AH66P cells rather than AH66DR cells.⁹ It is presumed that AH66DR cells may have a different mitochondrial function from that of AH66P cells as described previously by some investigators.²⁸⁻³⁰ Further studies will be necessary to elucidate a regulation of an antioxidant pathway at sites of free radical generation.

To investigate the intracellular traffic of the internalized conjugate, a change in M_r owing to degradation of the internalized BSA-conjugated [^{14}C]DXR was estimated in each subcellular fraction. The secondary lysosomal fraction mainly contained three peaks of ^{14}C compounds ranging from 3 to 70 kDa,

and M_r of ^{14}C compounds extracted from nuclear and from mitochondrial fractions was estimated to be smaller than 2 kDa. Contribution of the lysosomes in degradation of the conjugate has been demonstrated by us and some other investigators using lysosomotropic amines, such as ammonium chloride and chloroquine.^{9,31-33} In our present study, the essential contribution of the lysosomal degradation of the conjugate in exhibiting cytotoxicity was confirmed directly by the inhibitory effect on cell growth using DXR conjugation with isomeric poly-lysine. Although poly-D-lysine-conjugated DXR was taken up into the cells at almost the same ratio with poly-L-lysine-conjugated DXR, only poly-L-lysine-conjugated DXR exhibited the cytotoxicity because poly-L-lysine was digested by lysosomal enzymes, but poly-D-lysine was not.²⁰ The cytosolic fraction containing two peaks smaller than 2 kDa and larger than 500 kDa of [^{14}C]compounds suggested that the smaller compound may be released from lysosomes and the larger one may be a complex of BSA-conjugated DXR with tubulin^{34,35} or 'unknown' carrier protein. These results show that BSA-conjugated DXR taken up by endocytosis is degraded in lysosomes, and the resulting active adducts of DXR are released and distributed to target organelles.

The present investigation concluded that the lysosomal degradation of protein-conjugated DXR taken up by endocytosis, the so-called endocytic/lysosomal system and the liberation of the active adduct of DXR, must be essential stages in the expression of cytotoxicity. However, further intensive investigations are necessary to elucidate the precise role of protein-conjugated DXR in the expression of cytotoxicity against tumor cells, including MDR cells.

Acknowledgments

Authors thank Dr T Aoki for helpful discussion and Dr Y Tsukada for critical reading of the manuscript.

References

1. Chen CJ, Chin JE, Ueda K, *et al.* Internal duplication and homology with bacterial transport proteins in the *mdr1* (P-glycoprotein) gene from multidrug-resistant human cells. *Cell* 1986; **47**: 381-9.
2. Riordan JR, Deuchars K, Kartner N, *et al.* Amplification of P-glycoprotein genes in multidrug-resistant mammalian cell lines. *Nature* 1985; **316**: 817-9.
3. Tsuruo T, Iida H, Tsukagoshi S, *et al.* Increased accumulation of vincristine and adriamycin in drug-

- resistant P388 tumor cells following incubation with calcium antagonists and calmodulin inhibitors. *Cancer Res* 1982; **42**: 4730–3.
4. Twentyman PR, Fox NE, White DJG. Cyclosporin A and its analogues as modifiers of Adriamycin and vincristine resistance in a multi-drug resistant human lung cancer cell line. *Br J Cancer* 1987; **56**: 55–7.
5. Chen AY, Yu C, Potmesil M, et al. Camptothecin overcomes MDR1-mediated resistance in human KB carcinoma cells. *Cancer Res* 1991; **51**: 6039–44.
6. FitzGerald DJ, Willingham MC, Cardarelli CO, et al. A monoclonal antibody–*Pseudomonas* toxin conjugate that specifically kills multidrug-resistant cells. *Proc Natl Acad Sci USA* 1987; **84**: 4288–92.
7. Tsuruo T, Hamada H, Sato S, et al. Inhibition of multidrug-resistant human tumor growth in athymic mice by anti-P-glycoprotein monoclonal antibodies. *Jpn J Cancer Res* 1989; **80**: 627–31.
8. Pearson JW, Fogler WE, Volker K, et al. Reversal of drug resistance in a human colon cancer xenograft expressing MDR1 complementary DNA by *in vivo* administration of MRK-16 monoclonal antibody. *J Natl Cancer Inst* 1991; **83**: 1386–91.
9. Ohkawa K, Hatano T, Yamada K, et al. Bovine serum albumin–doxorubicin conjugate overcomes multidrug resistance in a rat hepatoma. *Cancer Res* 1993; **53**: 4238–42.
10. Ohkawa K, Hatano T, Tsukada Y, et al. Chemotherapeutic efficacy of the protein–doxorubicin conjugates on multidrug resistant rat hepatoma cell line *in vitro*. *Br J Cancer* 1993; **67**: 274–8.
11. Hatano T, Ohkawa K, Matsuda M. Cytotoxic effect of the protein–doxorubicin conjugates on the multidrug-resistant human Myelogenous leukemia cell line, K562, *in vitro*. *Tumor Biol* 1993; **14**: 288–94.
12. Ohkawa K, Hatano T, Takada K, et al. Monoclonal antibody against doxorubicin (DXR): some characteristics and utilization for DXR-immunoassay. *Int J Oncol* 1993; **3**: 43–6.
13. Hurwitz E, Levy R, Maron R, et al. The covalent binding of daunomycin and adriamycin to antibodies, with retention of both drug and antibody activities. *Cancer Res* 1975; **35**: 1175–81.
14. Tata JR. Biomembrane, part A. *Methods Enzymol* 1974; **31**: 253–62.
15. Mosmann T. Rapid colorimetric assay for cellular growth and survival: application to proliferation and cytotoxicity assays. *J Immunol Methods* 1983; **65**: 55–63.
16. Kissane JM, Robins E. The fluorimetric measurement of deoxyribonucleic acid in animal tissues with special reference to the central nervous system. *J Biol Chem* 1958; **233**: 184–8.
17. Morre DJ. Enzyme purification and related techniques. *Methods Enzymol* 1971; **22**: 130–48.
18. Shibko S, Tappel AL. Rat-kidney lysosomes: isolation and properties. *Biochem J* 1965; **95**: 731–41.
19. Bernstein LH, Everse J. Determination of isoenzyme levels of lactate dehydrogenase. *Methods Enzymol* 1975; **41**: 47–52.
20. Shen WC, Ryser HJP. Poly (L-Lysine) and poly (D-Lysine) conjugates of methotrexate; different inhibitory effect on drug resistant cells. *Mol Pharmacol* 1979; **16**: 614–22.
21. Baldini N, Scotlandi K, Shikita T, et al. Nuclear immunolocalization of P-glycoprotein in multidrug-resistant cell lines showing similar mechanisms of doxorubicin distribution. *Eur J Cell Biol* 1995; **68**: 226–39.
22. Liu LE. DNA topoisomerase poisons as antitumor drugs. *Annu Rev Biochem* 1989; **58**: 351–7.
23. Eijdem EWHM, de Haas M, Timmerman AJ, et al. Reduced topoisomerase II activity in multidrug-resistant human non-small cell lung cancer cell lines. *Br J Cancer* 1995; **71**: 40–7.
24. Hasegawa S, Abe T, Naito S, et al. Expression of multidrug resistance-associated protein (MRP), MDR1 and DNA topoisomerase II in human multidrug-resistant bladder cancer cell lines. *Br J Cancer* 1995; **71**: 907–13.
25. Bachur NR, Gordon SL, Gee MV. Anthracycline antibiotic augmentation of microsomal electron transport and free radical formation. *Mol Pharmacol* 1977; **13**: 901–10.
26. Kalyanaraman B, Perez-Reyes E, Mason RP. Spin-trapping and direct electron spin resonance investigations of the redox metabolism of quinone anticancer drugs. *Biochim Biophys Acta* 1980; **630**: 119–30.
27. Berlin V, Haseltine WA. Reduction of adriamycin to a semiquinone-free radical by NADPH cytochrome P-450 reductase produces DNA cleavage in a reaction mediated by molecular oxygen. *J Biol Chem* 1981; **256**: 4747–56.
28. Weaver JL, Pine PS, Aszalos A, et al. Laser scanning and confocal microscopy of daunorubicin, doxorubicin, and rhodamine 123 in multidrug-resistant cells. *Exp Cell Res* 1991; **196**: 323–9.
29. Hindenburg AA, Gervasoni JE Jr, Krishna S, et al. Intracellular distribution and pharmacokinetics of daunorubicin in anthracycline-sensitive and -resistant HL-60 cells. *Cancer Res* 1989; **49**: 4607–14.
30. Slapak CA, Lecerf JM, Daniel JC, et al. Energy-dependent accumulation of daunorubicin into subcellular compartments of human leukemia cells and cytoplasts. *J Biol Chem* 1992; **15**: 10638–44.
31. Shih LB, Goldenberg DM, Xuan H, et al. Internalization of an intact doxorubicin immunoconjugate. *Cancer Immunol Immunother* 1994; **38**: 92–8.
32. Basu S, Mukhopadhyay B, Basu SK, et al. Enhanced intracellular delivery of doxorubicin by scavenger receptor-mediated endocytosis for preferential killing of histiocytic lymphoma cells in culture. *FEBS Lett* 1994; **342**: 249–54.
33. Stahl P. Receptor-mediated endocytosis. In: Cuatrecasas P, Roth TF, eds. *Receptor and recognition*. B. London: Chapman & Hall 1983; **15**: 141–65.
34. Pineno HM, Giaccione G. P-glycoprotein—a marker of cancer-cell behavior. *New Engl J Med* 1995; **333**: 1417–9.
35. Reichle A, Diddens H, Altmayr F, et al. Beta-tubulin and P-glycoprotein: major determinants of vincristine accumulation in B-CLL cells. *Leukemia Res* 1995; **19**: 823–9.

(Received 8 June 1996; accepted 27 June 1996)